Cooperative Hybrid VLC-RF Systems for WSNs

Chao Zhang*, Jia Ye*, Jia Shi†, Gaofeng Pan*, Zan Li†, Zhiguo Ding†
*Chongqing Key Laboratory of Nonlinear Circuits and Intelligent Information Processing, SWU, Chongqing, 400715, China
†State key laboratory of integrated services networks, Xidian University, Xi'an, 710071, china.
‡School of Electrical and Electronic Engineering, University of Manchester, Manchester, M13 9PL, U.K.

***Abstract*—In this paper, a cooperative hybrid visible light communication (VLC)-radio frequency (RF) wireless sensor network, which includes a transmitter (S) with a cluster of light emitting diodes (LED) lamps, a relay (R) and a destination (D), is taken into consideration. Specially, R is randomly located in the coverage of the LED lamps, D is randomly distributed out of the coverage of the LED lamps. Then, VLC is employed for $S-R$ link and traditional radio frequency (RF) communication technology is adopted over $R-D$ link. Moreover, both of decode-forward (DF) and amplify-forward (AF) relay schemes are considered at R to aid the data transmissions between S and D. Considering Nakagami-m fading over $R-D$ link, and the randomness of the locations of R and D, the statistical characteristics of the received signal-to-noise ratio at D under both AF and DF relay schemes are characterized, respectively. After that, approximated analytical expressions for the outage probability of the considered system are respectively derived. Finally, simulation and numerical analysis are conducted to verify the correctness of our proposed analytical models.**

I. Introduction

To satisfy the rapid growth need in data transfer, visible light communication (VLC) has been regarded as an alternative supplement for traditional radio frequency (RF) communication technologies, as VLC can not only act as the function of illumination, but also provide high data rate transfer. More and more researchers put their eyes on the merits of VLC, such as nearly limitless bandwidth, low cost, high signal-to-noise ratio (SNR) and so on.

However, there are still some challenges met during implementing VLC in practical scenarios. For example, line-of-sight propagation is very crucial to VLC systems and hence the communications without LOS, such as sending signals across a wall or a few room, is impossible.

To enhance the performance of VLC systems, relays and RF communication have been presented as a promising method [3]-[7]. [3] proposed an angle diversity receivers relay, laser diodes (LDs) and select-the-best relay assisted LD-VLC system. [4] investigated the performance of cooperative VLC system with an intermediate light source served as a relay terminal. [5] considered a relay which can harvest energy from the received optical signal and then retransmit information to the destination. [6] studied the bit error rate performance of VLC systems where one task light served as a relay and an information source. [7] investigated the secrecy outage performance of a hybrid VLC-RF system where the terminal can retransmit information by using the energy harvested from light emitting diodes (LED) lamps.

Clearly, most of the researches related to VLC only focus on the systems with fixed position terminals, which is impractical in real world. In practical scenarios, the receivers may have mobility or be randomly deployed. Therefore, considering the the randomness of the locations of the terminals will be significant during the performance modeling and optimization processes. The authors of [7] and [8] studied the secrecy performance of indoor VLC systems with randomly distributed legitimate receiver and eavesdroppers by using stochastic geometry theory.

Motivated by all observations above, in this paper a hybrid VLC-RF wireless sensor network (WSN) system, which consists of a source (S) with a cluster of LEDs, a relay (R) and a destination (D), is considered. Particularly, photodiodes (PD) are adopted at R to receive the VLC signal, while traditional RF antenna is also used at R to deliver the received information from R to D. Then, the coverage of S can be extended. Then, in this way the shortage of pure VLC systems can be readily overcome. More specially, in this work we concentrate on the outage performance of the considered cooperative hybrid VLC-RF system, while both of AF and DF relay schemes are employed at R, respectively. Considering the randomness of the positions of both R and D, we derive the approximated analytical expressions for the outage probability (OP) of the target system.

II. System Model

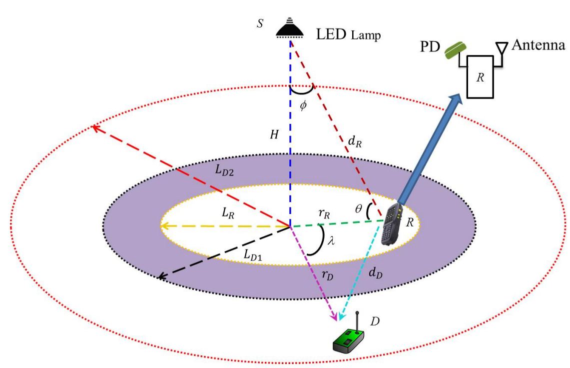

Fig. 1. System model

In this paper, we consider a cooperative hybrid VLC−RF WSN, as shown in Fig. 1, which consists of S with multiple LED lamps, R and D. We assume that AF and DF relay schemes are adopted at R to assist the information transmission between S and D. In detail, D is located out of the coverage of S, then R is employed to forward the information bits, while it is assumed that PD is adopted at R to receive the VLC signal transmitted by S, and traditional RF antenna is also used at R to deliver information from R to D. We also assume that the RF fading channel between R and D suffers Nakagami-m fading.

In this paper, it is assumed that R and D are uniformly distributed. In detail, R is randomly distributed in the circle with the radius L_R m ($L_R > 0$) and D is randomly placed in a ring with inner radius L_{D1} m and outer radius L_{D2} m. Without losing generality, we set $L_{D2} > L_{D1} >> L_R > 0$. To speak of the geometric relationship among LED lamps, R and D, the LED lamps are above the surface, where the circle of R and the ring of D are coplanar, and the height of S (the LED lamps) is H ($H > 0$) m, and the projection of the LED lamps is located at the center of the circle and the ring. We define the distance from the center to R as r_R, the one from the center to D as r_D, the one between S and R as d_R and the one between R and D as d_D.

We assume that there are N ($N > 1$) LED lamps transmitting information bits by using visible light signal to R, and all lamps are identical. It is also assumed that the distance between the ith LED lamp and R is $d_R = \sqrt{H^2 + r_R^2}$ to simplify the analysis, as all LED lamps are close to each other and the area of the PD at the LED lamps is normally on the order of 1 cm^2. Thus, as suggested by Eq. (4) in [7], the received RF power from the ith lamp at R can be written as

$$P_{i,R} = C_{RF} P_t^2 \cos^{2m_t}\phi / d_R^4, \tag{1}$$

where P_t is the optical transmit power at each lamp, $m_t = -\ln 2/\ln\left[\cos\left(\phi_{1/2}\right)\right]$ in which $\phi_{1/2}$ is the semi-angle of the LED, C_{RF} is RF power constant.

A. SNR under DF relay scheme

Using maximal-ratio combining (MRC) scheme and considering $\cos^{m_t}\phi = H/\left(H^2 + r_R^2\right)$, the received SNR at R can be presented as

$$\gamma_{OR} = \sum_{i=1}^{N} \frac{P_{i,R}}{N_0} = \lambda (H^2 + r_R^2)^{-(m_t+2)}, \tag{2}$$

where $\lambda = N C_{RF} P_t^2 H^{2m_t} / N_0$.

As R and D are uniformly distributed, we can derive the CDF of r_R as $P(x) = \int_0^{2\pi}\int_0^{x} \frac{1}{\pi L_R^2} r dr d\theta = \frac{x^2}{L_R^2}$. Then, the PDF of r_R can be obtained as $f(x) = 2x/L_R^2$, $0 \le x \le L_R$.

Therefore, the CDF and PDF of γ_{OR} can be given as

$$F_{\gamma_{OR}}(x) = 1 + \frac{H^2}{L_R^2} - \frac{\lambda^{\frac{1}{(m_t+2)}}}{L_R^2 x^{\frac{1}{m_t+2}}} \tag{3}$$

and

$$f_{\gamma_{OR}}(x) = \frac{\lambda^{\frac{1}{m_t+2}} x^{-\frac{m_t+3}{m_t+2}}}{(m_t+2) L_R^2}, \tag{4}$$

respectively.

Since traditional RF communication technology is adopted over the link from R to D, we can easily write the received signal at D as $y_{DF} = \sqrt{\frac{P_2}{d_D^n}} h_D x_R + z$, where P_2 is the transmit power at R, z is the complex Gaussian noise with zero means and the variance N_0, $|h_D|^2$ is the Nakagami-m fading gain, the probability distribution function (PDF) and cumulative distribution function (CDF) of which can be expressed as $f(x) = \frac{m^m x^{m-1}}{\Omega^m \Gamma(m)} \exp\left(-\frac{mx}{\Omega}\right)$ and $F(x) = \frac{1}{\Gamma(m)}\gamma(m, \frac{mx}{\Omega})$, respectively, where $\Gamma(\cdot)$ is the complete gamma function, $\gamma(\cdot,\cdot)$ is the lower incomplete gamma function, $\Omega = E\left[|h_D|^2\right]$, and $m = \frac{E^2\left[|h_D|^2\right]}{\mathrm{var}\left\{|h_D|^2\right\}}$.

In the considered model, it is easy to obtain $r_D \ge L_{D1} >> L_R \ge r_R$, then we can have $d_D = \sqrt{{r_R}^2 + {r_D}^2} \approx r_D$. Thus, the received SNR at D can be written as $\gamma_{RD} = \frac{P_2 |h_D|^2}{d_D^n N_0} \approx \frac{P_2 |h_D|^2}{r_D^n N_0}$.

Therefore, the end-to-end SNR under DF relay scheme can be derived as $\gamma_{DF} = \min(\gamma_{OR}, \gamma_{RD})$.

B. SNR under AF relay scheme

When AF relay scheme is utilized at R, R amplifies the received signal and forwards it to D by using the transmit power P_2.

Then, the received signal at D can be expressed as

$$\begin{aligned} y_{AF} &= G h_D \sqrt{\frac{1}{d_D^n}} y_R + z_2 \\ &= G h_D \sqrt{\frac{1}{d_D^n}} (P_t h_R x + z_1) + z_2, \end{aligned} \tag{5}$$

where the normalized power $G = \sqrt{\frac{P_2}{P_R + N_0}}$, h_R and h_D are channel gains from lamp to R and R to D, respectively. z_1 and z_2 are independent complex Gaussian noise with zero mean and variances N_0.

Similar with derivation in last subsection, the received SNR under AF relay scheme can be approximated as

$$\gamma_{AF} \approx \frac{P_2 |h_D|^2 P_R}{P_2 |h_D|^2 N_0 + d_D^n (P_R + N_0) N_0}, \tag{6}$$

where $P_R = N_0 \lambda (H^2 + r_R^2)^{-(m_t+2)}$.

III. Outage Analysis

In this section, we will derive the analysis expressions of the OP under DF and AF relay schemes, respectively.

A. Outage analysis under DF relay scheme

Considering $r_D \approx d_D$, and the two hops in the target system are independent with each other. Thus, OP can be given as

$$\begin{aligned} P_{out,DF} &= \Pr\left\{\min(\gamma_{OR}, \gamma_{RD}) < \gamma_{th,DF}\right\} \\ &= F_{\gamma_{OR}}(\gamma_{th,DF}) + F_{\gamma_{RD}}(\gamma_{th,DF}) \\ &\quad - F_{\gamma_{OR}}(\gamma_{th,DF}) F_{\gamma_{RD}}(\gamma_{th,DF}), \end{aligned} \tag{7}$$

where $\gamma_{th,DF}$ means the threshold value, $F_{\gamma_{OR}}(\cdot)$ is the CDF of γ_{OR} and $F_{\gamma_{RD}}(\cdot)$ is the CDF of γ_{RD}.

In order to obtain the analytical expression of OP, we should first derive the CDF of γ_{OR} and γ_{RD}, respectively. As the CDF of γ_{OR} has been calculated as (3). So, we need only calculate the CDF of γ_{RD}.

As the PDF of r_D can be written as $f(x) = 1\big/\left(\pi\left(L_{D2}^2 - L_{D1}^2\right)\right)$, the CDF of r_D can be given as

$$\begin{aligned} F_{r_D}(x) &= \int_0^{2\pi}\int_0^x \frac{1}{\pi\left(L_{\mathrm{D2}}^2 - L_{\mathrm{D1}}^2\right)} r dr d\theta \\ &= \frac{x^2}{L_{\mathrm{D2}}^2 - L_{\mathrm{D1}}^2}. \end{aligned} \tag{8}$$

Using (8), we can easily derive the CDF of $\frac{N_0 r_D^n}{P_2}$ as

$$\begin{aligned} F_{\frac{N_0 r_D^n}{P_2}}(x) &= \Pr\left\{\frac{N_0 r_D^n}{P_2} < x\right\} \\ &= \Pr\left\{r_D < \sqrt[n]{\frac{P_2 x}{N_0}}\right\} \\ &= \left(\frac{P_2}{N_0}\right)^{\frac{2}{n}} \frac{x^{\frac{2}{n}}}{L_{\mathrm{D2}}^2 - L_{\mathrm{D1}}^2}. \end{aligned} \tag{9}$$

Then, the PDF of $\frac{N_0 r_D^n}{P_2}$ can be easily obtained as

$$f_{\frac{N_0 r_D^n}{P_2}}(x) = \left(\frac{P_2}{N_0}\right)^{\frac{2}{n}} \frac{2x^{\frac{2}{n}-1}}{n\left(L_{\mathrm{D2}}^2 - L_{\mathrm{D1}}^2\right)}. \tag{10}$$

Because $\gamma_{RD} = |h_D|^2\Big/\left(\frac{N_0 r_D^n}{P_2}\right)$, we can express the PDF of γ_{RD} as

$$\begin{aligned} f_{\gamma_{RD}}(x) &= \int_0^\infty y f_{|h_D|^2}(yx) f_{\frac{N_0 r_D^n}{P_2}}(y)\, dy \\ &= \frac{2x^{m-1}}{n\left(L_{\mathrm{D2}}^2 - L_{\mathrm{D1}}^2\right)\Gamma(m)}\left(\frac{m}{\Omega}\right)^m \left(\frac{P_2}{N_0}\right)^{\frac{2}{n}} \\ &\quad \cdot \underbrace{\int_{a_1}^{b_1} y^{\frac{2}{n}+m-1}\exp\left(-\frac{mxy}{\Omega}\right) dy}_{\mathrm{I}_1}, \end{aligned} \tag{11}$$

where $\Gamma(\cdot)$ means gamma function, $a_1 = \left(\frac{N_0 L_{D1}^n}{P_2}\right)$ and $b_1 = \left(\frac{N_0 L_{D2}^n}{P_2}\right)$.

I_1 in last equation can be calculated as

$$\begin{aligned} \mathrm{I}_1 &= \int_{a_1}^{b_1} t^{\frac{2}{n}+m-1}\exp\left(-\frac{mxt}{\Omega}\right) dt \\ &= \int_0^{b_1} t^{\frac{2}{n}+m-1}\exp\left(-\frac{mxt}{\Omega}\right) dt \\ &\quad - \int_0^{a_1} t^{\frac{2}{n}+m-1}\exp\left(-\frac{mxt}{\Omega}\right) dt \\ &= \left(\frac{\Omega}{mx}\right)^{\frac{2}{n}+m}\gamma\left(\frac{2}{n}+m, \frac{mxb_1}{\Omega}\right) \\ &\quad - \left(\frac{\Omega}{mx}\right)^{\frac{2}{n}+m}\gamma\left(\frac{2}{n}+m, \frac{mxa_1}{\Omega}\right), \end{aligned} \tag{12}$$

where $\gamma(\cdot,\cdot)$ means the lower incomplete gamma function.

Therefore, substituting (12) into (11), we can derive the PDF of γ_{RD} as

$$\begin{aligned} f_{\gamma_{RD}}(x) &= \frac{\Theta}{x^{\frac{2}{n}+1}}\gamma\left(\frac{2}{n}+m, \frac{mxb_1}{\Omega}\right) \\ &\quad - \frac{\Theta}{x^{\frac{2}{n}+1}}\gamma\left(\frac{2}{n}+m, \frac{mxa_1}{\Omega}\right), \end{aligned} \tag{13}$$

where $\Theta = \frac{2}{n\left(L_{\mathrm{D2}}^2 - L_{\mathrm{D1}}^2\right)\Gamma(m)}\left(\frac{\Omega}{m}\right)^{\frac{2}{n}}\left(\frac{P_2}{N_0}\right)^{\frac{2}{n}}$.

So the CDF of γ_{RD} can be given as

$$\begin{aligned} F_{\gamma_{RD}}(x) &= \int_0^x \frac{\Theta}{y^{\frac{2}{n}+1}}\gamma\left(\frac{2}{n}+m, \frac{mb_1 y}{\Omega}\right) dy \\ &\quad - \int_0^x \frac{\Theta}{y^{\frac{2}{n}+1}}\gamma\left(\frac{2}{n}+m, \frac{ma_1 y}{\Omega}\right) dy. \end{aligned} \tag{14}$$

In order to obtain the CDF of γ_{RD}, in the following we define a new function I_2 and using Eq.[2.10.2.2] in [11], we can have

$$\begin{aligned} \mathrm{I}_2 &= \int_0^x y^{-\left(\frac{2}{n}+1\right)}\gamma\left(\frac{2}{n}+m, \frac{mb_1 y}{\Omega}\right) dy \\ &\quad - \int_0^x y^{-\left(\frac{2}{n}+1\right)}\gamma\left(\frac{2}{n}+m, \frac{ma_1 y}{\Omega}\right) dy \\ &= \left(\frac{2}{n}+m\right)^{-1}\left(\frac{mb_1}{\Omega}\right)^{\frac{2}{n}+m} x^m \mathrm{B}(1,m) \\ &\quad \cdot {}_2F_2\left(\frac{2}{n}+m, m; \frac{2}{n}+m+1, m+1; \frac{-mb_1 x}{\Omega}\right) \\ &\quad - \left(\frac{2}{n}+m\right)^{-1}\left(\frac{ma_1}{\Omega}\right)^{\frac{2}{n}+m} x^m \mathrm{B}(1,m) \\ &\quad \cdot {}_2F_2\left(\frac{2}{n}+m, m; \frac{2}{n}+m+1, m+1; \frac{-ma_1 x}{\Omega}\right), \end{aligned} \tag{15}$$

where $\mathrm{B}(\cdot,\cdot)$ denotes the beta function and ${}_2F_2(\cdot,\cdot;\cdot,\cdot;\cdot)$ is the hypergeometric function.

Then, the CDF of γ_{RD} can be written as

$$F_{\gamma_{RD}}(x) = \Theta \mathrm{I}_2. \tag{16}$$

Finally, we can obtain the analysis expression of the OP under DF relay scheme by substituting (3) and (16) into (7).

B. Outage analysis under AF relay scheme

As $r_D \approx d_D$, OP under AF relay scheme can be derived as

$$\begin{aligned} P_{out,AF} &= \Pr\left\{\gamma_{D,AF} < \gamma_{th}\right\} \\ &= \Pr\left\{\frac{P_2 |h_D|^2 P_R}{P_2 |h_D|^2 N_0 + d_D^n\left(P_R + N_0\right) N_0} < \gamma_{th}\right\} \\ &= \Pr\left\{\frac{P_2 |h_D|^2}{\gamma_{th} d_D^n N_0} < \frac{P_R + N_0}{P_R - \gamma_{th} N_0}\right\} \\ &\approx \Pr\left\{\underbrace{\frac{P_2 |h_D|^2}{\gamma_{th} r_D^n N_0}}_{X} < 1 + \underbrace{\frac{N_0\left(1+\gamma_{th}\right)}{P_R - \gamma_{th} N_0}}_{Y}\right\}, \end{aligned} \tag{17}$$

where $X = \frac{P_2|h_D|^2}{\gamma_{th} r_D^n N_0}$ and $Y = \frac{N_0(1+\gamma_{th})}{P_R-\gamma_{th}N_0}$.

On account of the PDF of r_D, the PDF of $\gamma_{th}N_0 r_D^n/P_2$ can be easily achieved as

$$f_{\frac{\gamma_{th}N_0 r_D^n}{P_2}}(x) = \frac{2x^{\frac{2}{n}-1}}{n\left(L_{D2}^2 - L_{D1}^2\right)}\left(\frac{P_2}{\gamma_{th}N_0}\right)^{\frac{2}{n}}. \tag{18}$$

We set $Q = \frac{N_0\gamma_{th}r_D^n}{P_2}$ and $P = |h_D|^2$, so $X = P/Q$. Due to the independence of P and Q, the PDF of X can be calculated as

$$\begin{aligned} f_X(x) &= \int_0^\infty y f_P(yx) f_Q(y) dy \\ &= \frac{2x^{m-1}}{n\left(L_{\mathrm{D2}}^2 - L_{\mathrm{D1}}^2\right)\Gamma(m)}\left(\frac{m}{\Omega}\right)^m\left(\frac{P_2}{N_0\gamma_{th}}\right)^{\frac{2}{n}} \\ &\quad\cdot \int_a^b y^{\frac{2}{n}+m-1}\exp\left(-\frac{mxy}{\Omega}\right)dy \\ &= \Lambda x^{m-1}\int_a^b y^{\frac{2}{n}+m-1}\exp\left(-\frac{mxy}{\Omega}\right)dy, \end{aligned} \tag{19}$$

where $\Lambda = \frac{2}{n\left(L_{\mathrm{D2}}^2-L_{\mathrm{D1}}^2\right)\Gamma(m)}\left(\frac{m}{\Omega}\right)^m\left(\frac{P_2}{N_0\gamma_{th}}\right)^{\frac{2}{n}}$, $a = \left(\frac{\gamma_{th}N_0L_{D1}^n}{P_2}\right)$ and $b = \left(\frac{\gamma_{th}N_0L_{D2}^n}{P_2}\right)$.

It is easy to rewrite $Y = \frac{N_0(1+\gamma_{th})}{P_R-\gamma_{th}N_0} = \frac{1+\gamma_{th}}{\gamma_{OR}-\gamma_{th}}$. Therefore, using (3), we can derive the CDF and PDF of Y as

$$\begin{aligned} F_Y(x) &= \Pr\{\frac{1+\gamma_{th}}{\gamma_{OR}-\gamma_{th}} < x\} \\ &= 1 - \Pr\{\gamma_{OR} < \frac{1+\gamma_{th}}{x} + \gamma_{th}\} \\ &= -\frac{H^2}{L_R^2} + \frac{\lambda^{\frac{1}{m_t+2}}}{L_R^2}\left(\frac{1+\gamma_{th}}{x}+\gamma_{th}\right)^{-\frac{1}{m_t+2}} \end{aligned} \tag{20}$$

and

$$\begin{aligned} f_Y(x) &= \frac{\lambda^{\frac{1}{m_t+2}}(1+\gamma_{th})}{(m_t+2)L_R^2x^2}\left(\frac{1+\gamma_{th}}{x}+\gamma_{th}\right)^{-\frac{m_t+3}{m_t+2}} \\ &= \frac{\Xi}{x^2}\left(\frac{1+\gamma_{th}}{x}+\gamma_{th}\right)^{-\frac{m_t+3}{m_t+2}}, \end{aligned} \tag{21}$$

respectively, where $\Xi = \frac{\lambda^{\frac{1}{m_t+2}}(1+\gamma_{th})}{L_R^2(m_t+2)}$.

In the following, we can rewrite (17) as

$$\begin{aligned} P_{out,AF} &= \Pr\{X < 1+Y, c_1 < Y < c_2, X > 0\} \\ &= \int_{c_1}^{c_2}\int_0^{1+y}\Lambda x^{m-1} \\ &\quad \underbrace{\cdot\int_a^b t^{\frac{2}{n}+m-1}\exp\left(\frac{-mxt}{\Omega}\right)dt}_{\mathrm{I}_1'}\, dx\, f_Y(y)\, dy, \end{aligned} \tag{22}$$

where $c_1 = \frac{\gamma_{th}+1}{\lambda H^{-2(m_t+2)}-\gamma_{th}}$ and $c_2 = \frac{\gamma_{th}+1}{\lambda(H^2+L_R^2)^{-(m_t+2)}-\gamma_{th}}$.

Although I_1' has different integration range comparing to I_1, the integral form of I_1' is similar with the one of I_1. Then, the method adopted to calculate I_1 can also be utilized here.

Therefore, making use of (12), and substituting (12) into (22) and changing the integration range, OP can be rewritten as

$$P_{out,AF} = \int_{c_1}^{c_2}\Lambda\left(\frac{\Omega}{m}\right)^{\frac{2}{n}+m}\mathrm{I}_3 f_Y(y)dy \tag{23}$$

where $\mathrm{I}_3 = \int_0^{1+y} x^{-\left(\frac{2}{n}+1\right)}\left[\gamma\left(\frac{2}{n}+m, \frac{mxb}{\Omega}\right) - \gamma\left(\frac{2}{n}+m, \frac{mxa}{\Omega}\right)\right] dx$.

Further, using Eq.[2.10.2.2] in [11], I_3 can be written as

$$\begin{aligned} \mathrm{I}_3 = &\left(\frac{2}{n}+m\right)^{-1}\left(\frac{mb}{\Omega}\right)^{\frac{2}{n}+m}(1+y)^m\mathrm{B}(1,m) \\ &\cdot {}_2F_2\left(\frac{2}{n}+m, m; \frac{2}{n}+m+1, m+1; \frac{-mb(1+y)}{\Omega}\right) \\ &- \left(\frac{2}{n}+m\right)^{-1}\left(\frac{ma}{\Omega}\right)^{\frac{2}{n}+m}(1+y)^m\mathrm{B}(1,m) \\ &\cdot {}_2F_2\left(\frac{2}{n}+m, m; \frac{2}{n}+m+1, m+1; \frac{-ma(1+y)}{\Omega}\right). \end{aligned} \tag{24}$$

Substituting (24) into (23), we can rewrite OP as

$$\begin{aligned} P_{out,AF} &= \Lambda\Xi\left(\frac{\Omega}{m}\right)^{\frac{2}{n}+m}\int_{c_1}^{c_2}\frac{\mathrm{I}_3}{y^2}\left(\frac{1+\gamma_{th}}{y}+\gamma_{th}\right)^{-\frac{m_t+3}{m_t+2}}dy \\ &= \Lambda\Xi\left(\frac{\Omega}{m}\right)^{\frac{2}{n}+m}(\mathrm{I}_4 - \mathrm{I}_5), \end{aligned} \tag{25}$$

where I_4 and I_5 can be expressed as

$$\begin{aligned} \mathrm{I}_4 = &\left(\frac{2}{n}+m\right)^{-1}\left(\frac{mb}{\Omega}\right)^{\frac{2}{n}+m}\mathrm{B}(1,m) \\ &\cdot\int_{c_1}^{c_2} {}_2F_2\left(\frac{2}{n}+m, m; \frac{2}{n}+m+1, m+1; \frac{-mb(1+y)}{\Omega}\right) \\ &\cdot y^{-2}(1+y)^m\left(\frac{1+\gamma_{th}}{y}+\gamma_{th}\right)^{-\frac{m_t+3}{m_t+2}}dy \end{aligned} \tag{26}$$

and

$$\begin{aligned} \mathrm{I}_5 = &\left(\frac{2}{n}+m\right)^{-1}\left(\frac{ma}{\Omega}\right)^{\frac{2}{n}+m}\mathrm{B}(1,m) \\ &\cdot\int_{c_1}^{c_2} {}_2F_2\left(\frac{2}{n}+m, m; \frac{2}{n}+m+1, m+1; \frac{-ma(1+y)}{\Omega}\right) \\ &\cdot y^{-2}(1+y)^m\left(\frac{1+\gamma_{th}}{y}+\gamma_{th}\right)^{-\frac{m_t+3}{m_t+2}}dy, \end{aligned} \tag{27}$$

respectively.

Then, in the following we can calculate I_4 and I_5, respectively. Using Chebyshev-Gauss quadrature in the first case which is given as $\int_{-1}^{+1}\frac{f(x)}{\sqrt{1-x^2}}dx \approx \sum_{i=1}^{S} w_i f(x_i)$ with $w_i = \pi/S$ and $x_i = \cos\left(\frac{2i-1}{2S}\pi\right)$, I_4 and I_5 can be respectively rewritten as the expression on the top of next page, where $d_1 = \frac{c_2-c_1}{2}$, $d_2 = \frac{c_2+c_1}{2}$, $\Psi = d_1\left(\frac{2}{n}+m\right)^{-1}\left(\frac{m}{\Omega}\right)^{\frac{2}{n}+m}\mathrm{B}(1,m)$, $W_i = \pi/I$, $\phi_i = \cos\left(\frac{2i-1}{2I}\pi\right)$, $W_j = \pi/J$ and $\tau_j = \cos\left(\frac{2j-1}{2J}\pi\right)$

Finally, the OP under AF relay scheme can be achieved by substituting (28) and (29) into (25).

$$
\begin{aligned}
\mathrm{I}_4 &= \Psi b^{\frac{2}{n}+m} \int_{-1}^{1} {}_2F_2\left(\frac{2}{n}+m, m; \frac{2}{n}+m+1, m+1; \frac{-mb\left(1+d_1t+d_2\right)}{\Omega}\right) \\
&\quad \cdot (d_1t+d_2)^{-2}(1+d_1t+d_2)^m \left(\frac{1+\gamma_{th}}{d_1t+d_2}+\gamma_{th}\right)^{-\frac{m_t+3}{m_t+2}} dt \\
&= \Psi b^{\frac{2}{n}+m} \sum_{i=1}^{I} W_i \sqrt{1-{\phi_i}^2}\, {}_2F_2\left(\frac{2}{n}+m, m; \frac{2}{n}+m+1, m+1; \frac{-mb\left(1+d_1\phi_i+d_2\right)}{\Omega}\right) \\
&\quad \cdot (d_1\phi_i+d_2)^{-2}(1+d_1\phi_i+d_2)^m \left(\frac{1+\gamma_{th}}{d_1\phi_i+d_2}+\gamma_{th}\right)^{-\frac{m_t+3}{m_t+2}}
\end{aligned} \tag{28}
$$

$$
\begin{aligned}
\mathrm{I}_5 &= \Psi a^{\frac{2}{n}+m} \sum_{j=1}^{J} W_j \sqrt{1-{\tau_j}^2}\, {}_2F_2\left(\frac{2}{n}+m, m; \frac{2}{n}+m+1, m+1; \frac{-ma\left(1+d_1\tau_j+d_2\right)}{\Omega}\right) \\
&\quad \cdot (d_1\tau_j+d_2)^{-2}(1+d_1\tau_j+d_2)^m \left(\frac{1+\gamma_{th}}{d_1\tau_j+d_2}+\gamma_{th}\right)^{-\frac{m_t+3}{m_t+2}}
\end{aligned} \tag{29}
$$

IV. Numerical Results and Discussions

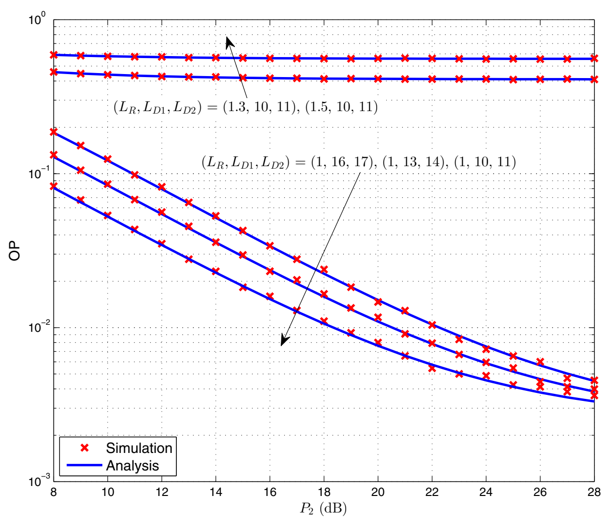

Fig. 2. OP v.s. P_2 for various L_R, L_{D1} and L_{D2} under DF scheme

A. DF relay scheme

In this subsection, we consider the scenarios under DF relay scheme with various system settings. Unless otherwise explicitly specified, parameters are set as: the transmit power at each LED lamp $P_t = 2$ W, the number of LED lamp $N = 16$, the transmit power at R under DF relay scheme $P_2 = 8$ W, $H = 3$ m, $L_R = 1$ m, $L_{D1} = 10$ m, $L_{D2} = 11$ m, $\gamma_{th} = 0$ dB, $m = 1$ m, $\Omega = -10$ dB. Simulations are performed by transmitting 1×10^5 bits.

In Fig. 2, we presents simulation and analytical results of OP v.s. P_2 for various combinations of (L_R, L_{D1}, L_{D2}), while $N_0 = -3.31$ dB and $m = 1$. One can observe that the OP with low L_R outperforms the one with high L_R due to the reason that the signal suffers small pathloss while being transmitted over short distance from S to R. When L_{D1} and L_{D2} vary, long $R - D$ link contributes to more severe fading, resulting in low SNR.

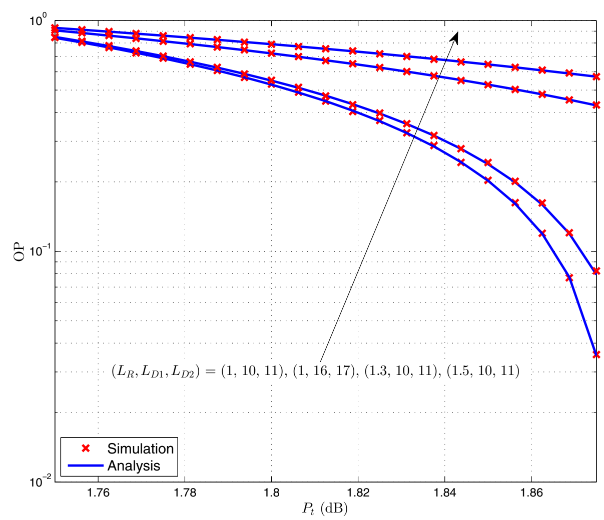

Fig. 3. OP v.s. P_t for various L_R, L_{D1} and L_{D2} under DF scheme

Fig. 3 depicts simulation and analytical results of OP v.s. P_t for various combinations of (L_R, L_{D1}, L_{D2}), while $N_0 = -6.37$ dB and $m = 1$. When L_R varies, it is significant to achieve that smaller L_R leads to lower OP. Because when the fading distance between S and R declines, the received power of the signals at R will increase fast, leading to high SNR. While changing L_{D1} and L_{D2}, the OP with high L_{D1} and

L_{D2} outperforms the one with low L_R, for the reason that long distance from R to D causes low SNR.

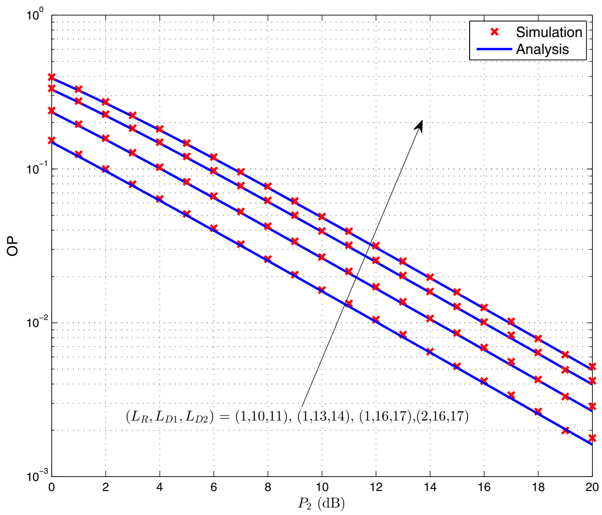

Fig. 4. OP v.s. P_2 for various L_R, L_{D1} and L_{D2} under AF sceme

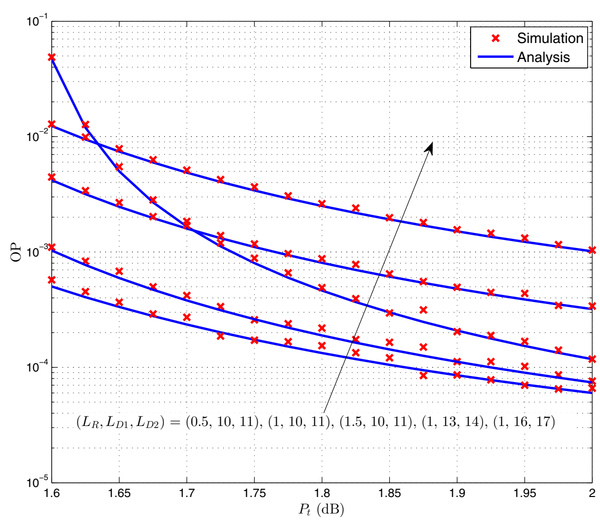

Fig. 5. OP v.s. P_t for various L_R, L_{D1} and L_{D2} under AF scheme

B. AF relay scheme

In the following, we will discuss the target system with AF relay scheme. Unless otherwise explicitly specified, we adopt the same setting for the parameters as the one for the parameters under DF relay scheme in last subsection besides $N_0 = -10$ dB.

In Fig. 4, simulation and analytical results of OP v.s. P_2 for various combination parameters (L_R, L_{D1}, L_{D2}) are presented. Obviously, it is easy to obtain that large L_R means high OP, because when the fading distance between S and R, d_R, increases, the received power of the signals at R declines fast, leading to the low SNR. One can also observe that the OP of low L_{D1} and L_{D2} outperforms the one with high L_{D1} and L_{D2} for the reason that lower distance from the R to D, d_D, implies higher SNR under AF relay scheme.

Fig. 5 presents simulation and analytical results of OP v.s. P_t for various combination parameters (L_R, L_{D1}, L_{D2}). On the one hand, the OP with high L_R performs worse than the one with low L_R, due to the reason that the signals are transmitted over longer distance from S to R, d_R, and suffers more serious fading, further resulting in lower SNR. On the other hand, the OP with low L_{D1} and L_{D2} outperforms the one with high L_{D1} and L_{D2}. Because the distance from R and D, d_D, influences SNR seriously, and the higher d_D is, the lower SNR is.

V. Conclusion

In this paper, we have studied the outage performance of cooperative hybrid VLC-RF WSN under DF and AF relay schemes, respectively. By considering the randomness of the positions of R and D, the approximated expressions for OP have been respectively derived and verified via Monte Carlo simulations.

VI. Acknowledgment

This research was supported by the Royal Society International Exchange Scheme and the UK EPSRC under grant number EP/N005597/1.

References

[1] F. Miramirkhani, O. Narmanlioglu, M. Uysal and E. Panayirci, “A mobile channel model for VLC and application to adaptive system design,” *IEEE Commun. Lett.*, vol. 21, no. 5, pp. 1035-1038, May. 2017.

[2] B. Li, J. Wang, R. Zhang, H. Shen, C. Zhao and L. Hanzo, “Multiuser MISO transceiver design for indoor downlink visible light communication under per-LED optical power constraints,” *IEEE Photon. J.*, vol. 7, no. 4, pp. 1-15, Aug. 2015.

[3] A. T. Hussein and J. M. H. Elmirghani, “10 Gbps mobile visible light communication system employing angle diversity, imaging receivers, and relay nodes,” *IEEE/OSA J. Opt. Commun. Netw.*, vol. 7, no. 8, pp. 718-735, Aug. 2015.

[4] O. Narmanlioglu, R. C. Kizilirmak, F. Miramirkhani and M. Uysal, “Cooperative visible light communications with full-duplex relaying,” *IEEE Photon. J.*, vol. 9, no. 3, pp. 1-11, Jun. 2017.

[5] T. Rakia, H. C. Yang, F. Gebali and M. S. Alouini, “optimal design of dual-hop VLC/RF communication system with energy harvesting,” *IEEE Commu. Lett.*, vol. 20, no. 10, pp. 1979-1982, Oct. 2016.

[6] R. C. Kizilirmak, O. Narmanlioglu and M. Uysal, “Relay-assisted OFDM-based visible light communications,” *IEEE Trans. Commun.*, vol. 63, no. 10, pp. 3765-3778, Oct. 2015.

[7] G. Pan, J. Ye and Z. Ding, “Secure hybrid VLC-RF systems with light energy harvesting,” *IEEE Trans. Commun.*, vol. 65, no. 10, pp. 4348-4359, Oct. 2017.

[8] G. Pan, J. Ye and Z. Ding, “On secure VLC systems with spatially random terminals,” *IEEE Commu. Lett.*, vol. 21, no. 3, pp. 492-495, Mar. 2017.

[9] A. P. Prudnikov, Yu. A. Brychkov, and O. I. Marichev, *Integrals and series, vol. 3, More Special Functions*. New York: Gordon & Breach Sci. Publ., 1986.

[10] A. P. Prudnikov, Yu. A. Brychkov, and O. I. Marichev, *Integrals and series, vol. 1, Elementary Functions*. New York: Gordon & Breach Sci. Publ., 1986.

[11] A. P. Prudnikov, Yu. A. Brychkov, and O. I. Marichev, *Integrals and series, vol. 2, special functions*. New York: Gordon & Breach Sci. Publ., 1986.